

MIF Produced by Bone Marrow–Derived Macrophages Contributes to Teratoma Progression after Embryonic Stem Cell Transplantation

Xi Wang^{1,6}, Tianxiang Chen^{1,7}, Lin Leng⁴, Jianqing Fan³, Kai Cao¹, Zhaoxia Duan^{1,9}, Xijing Zhang⁵, Changshun Shao², Mingmei Wu¹, Iman Tadmori¹, Tianyi Li¹, Li Liang², Dongming Sun¹, Shusen Zheng⁷, Andreas Meinhardt⁸, Wise Young¹, Richard Bucala², and Yi Ren¹

Abstract

Although stem cell therapy holds promise as a potential treatment in a number of diseases, the tumorigenicity of embryonic stem cells (ESC) and induced pluripotent stem cells remains a major obstacle. *In vitro* predifferentiation of ESCs can help prevent the risk of teratoma formation, yet proliferating neural progenitors can generate tumors, especially in the presence of immunosuppressive therapy. In this study, we investigated the effects of the microenvironment on stem cell growth and teratoma development using undifferentiated ESCs. Syngeneic ESC transplantation triggered an inflammatory response that involved the recruitment of bone marrow (BM)–derived macrophages. These macrophages differentiated into an M2 or angiogenic phenotype that expressed multiple angiogenic growth factors and proteinases, such as macrophage migration inhibitory factor (MIF), VEGF, and matrix metalloproteinase 9, creating a microenvironment that supported the initiation of teratoma development. Genetic deletion of MIF from the host but not from ESCs specifically reduced angiogenesis and teratoma growth, and MIF inhibition effectively reduced teratoma development after ESC transplantation. Together, our findings show that syngeneic ESC transplantation provokes an inflammatory response that involves the rapid recruitment and activation of BM-derived macrophages, which may be a crucial driving force in the initiation and progression of teratomas. *Cancer Res*; 72(11); 2867–78. ©2012 AACR.

Introduction

Stem cell therapy holds an enormous potential as a treatment for many diseases, including spinal cord injury. However, embryonic stem cells (ESC) and induced pluripotent stem (iPS) cells produce teratomas. The risk of teratoma development represents a major obstacle to successful clinical translation of stem cell therapies. Although teratoma formation can be

reduced by *in vitro* predifferentiation of ESCs, recent observation revealed that not only undifferentiated human ESCs (hESC) but also ESCs proliferating neural progenitors can generate tumors (1, 2), especially under the immunosuppressive treatment (3). Teratomas have been found also after injection of *in vitro* differentiated cells into various other tissues including liver and myocardium (4, 5). Human iPS cells are a potential source of patient-specific pluripotent stem cells and expected to have tremendous value for therapeutic purposes. However, it is inevitable that these iPS cells develop teratomas even if these iPS cells are predifferentiated *in vitro* still formed teratomas (6). Furthermore, some iPS-derived neurospheres showed robust teratoma formation (7, 8). The potential tumorigenicity must be evaluated directly before the clinical application of any stem cell in regenerative medicine (9, 10).

Teratoma development requires several molecular processes such as self-renewal, rapid proliferation, lack of contact inhibition, and telomerase activity (11, 12). The marker genes for hESCs and those required for the generation of iPS cells, including *Oct4*, *Sox2*, *Nanog*, *Lin28*, *Myc*, and *Klf4*, are linked to stem cell tumorigenesis (11). Many tumor suppresser genes are hypermethylated and silenced in hESCs (11). In addition, *Survivin*, an antiapoptotic gene, also contributes to hESC-induced teratoma formation (13). However, the mechanisms of teratoma development are complex and may require the presence of supporting host cells in the ESC microenvironment. Inflammation is a major driving force for the initiation

Authors' Affiliations: ¹W. M. Keck Center for Collaborative Neuroscience and ²Department of Genetics, Rutgers, The State University of New Jersey, Piscataway; ³Statistics Laboratory, Princeton University, Princeton, New Jersey; ⁴Department of Internal Medicine, Yale University School of Medicine, New Haven, Connecticut; ⁵Department of Anesthesiology, Xijing Hospital; ⁶Institute of Neuroscience, The Fourth Military Medical University, Xi'an; ⁷Department of Hepatobiliary and Pancreatic Surgery, First Affiliated Hospital, Zhejiang University, Hangzhou, China; ⁸Department of Anatomy and Cell Biology, Justus-Liebig-University Giessen, Giessen, Germany; ⁹Department 6, Research Institute of Surgery, Daping Hospital, Third Military Medical University, Chongqing, China

Note: Supplementary data for this article are available at Cancer Research Online (<http://cancerres.aacrjournals.org/>).

X. Wang and T. Chen contributed equally to this study.

Corresponding Author: Yi Ren, W. M. Keck Center for Collaborative Neuroscience, Rutgers, The State University of New Jersey, Nelson Labs D-251, 604 Allison Road, Piscataway, NJ 08854. Phone: 732-445-1786; Fax: 732-445-2063; E-mail: ren@dls.rutgers.edu

doi: 10.1158/0008-5472.CAN-11-3247

©2012 American Association for Cancer Research.

and progression of tumor development. Macrophage migration inhibitory factor (MIF) is important in the regulation of host inflammatory and immune responses but may be recognized as a protumorigenic factor (14) that is overexpressed in many tumors. We have previously shown that increased MIF expression in different cancers correlated significantly with unfavorable clinical outcomes (15, 16). Given the role of MIF in inflammation and tumor development, MIF may be an important link between inflammation and teratoma development.

In this study, we showed that syngeneic ESC transplantation provokes an inflammatory response that involves the rapid recruitment of bone marrow (BM)-derived macrophages; these cells created a microenvironment that facilitates the initiation and progression of teratomas. We found that ESCs recruit and activate macrophages that deliver MIF and other angiogenic factors to stimulate endothelial cell proliferation and pericyte differentiation. We further showed that MIF expressed by BM-derived macrophages (BMDM) is essential to teratoma growth and represents an important target to control teratoma development after ESC transplantation.

Materials and Methods

Mice strains

Wild-type (WT) C57BL/6 and C57BL/6-Tg(ACTB-mRFP1) 1F1Hadj/J mice "RFP mice" were purchased from Jackson Laboratory. MIF KO mice bred onto a pure C57BL/6 background (generation N10) have been described previously (17). All mice were maintained in pathogen-free animal facility at Rutgers University. Animal protocols were approved by Animal Care and Facilities Committee of Rutgers University.

Cells

Murine ESC line F12 from C57BL/6 mice ubiquitously expressing enhanced GFP (EGFP) under the control of the chicken actin promoter was used (18). ESCs, primary endothelial cells, and mouse BMDMs were prepared as described (18, 19) and additional methods are provided in the Supplementary Data.

Assays for cell proliferation, ELISA, histology, and immunofluorescence

The methodology for these assays is described in Supplementary Data.

Transplantation of EGFP-ESCs and MIF KO ESCs

Cell density in transplantation solutions was adjusted to 100,000 viable cells per microliter, and a total volume of 0.5 μ L was stereotaxically injected into the spinal cord of adult WT and MIF KO mice (8–12 weeks) at T9–T10 vertebrae by a T10 laminectomy with a microliter syringe (Hamilton Company) fixed in a stereotaxic frame. Mice were allowed to be sacrificed at different time points after transplantation. Functional assessment began on postoperative 24 hours as day 1. Hind limb motor function was assessed by the Basso Mouse Scale (BMS) score (20).

Angiogenesis in Matrigel plugs

Recombinant mouse VEGF-A (30 ng/mL; R&D Systems), heparin 60 U/mL, and bovine serum albumin 50 μ g/mL were

mixed with 250 μ L of regular Matrigel (BD Biosciences). The Matrigel (250 μ L each) was injected subcutaneously into the abdominal region of WT and MIF KO mice as described (21). Each Matrigel plug was harvested on day 5 and fixed in 4% paraformaldehyde and then cryoprotected in 20% sucrose overnight at 4°C before being sectioned for immunohistochemistry.

BM reconstitution

Eight-week-old mice as recipients were irradiated in a plastic box with 10 Gy. Subsequently, mice received an intravenous injection of 5×10^6 BM cells that had been harvested by flushing the marrow cavity of femurs of appropriate donor mice with Dulbecco's Modified Eagle's Medium (DMEM) supplemented with 1% FBS. The BM cells were washed several times with PBS and then contaminating red blood cells were lysed. The BM cells were resuspended in DMEM and injected intravenously via a tail vein with a 26-gauge needle. The chimeras created by this process were defined as follows: WT→WT: WT background irradiated, reconstituted with RFP-WT BM cells; WT→MIF KO: MIF KO mice irradiated, reconstituted with RFP-WT BM cells; MIF KO→WT: WT mice irradiated, reconstituted with MIF KO BM cells.

Treatment groups

WT mice inoculated with ESCs were randomly allocated into control and treatment groups. In the treatment groups, mice were administered neutralizing anti-MIF monoclonal antibody (mAb; 20 mg/kg) or control immunoglobulin G (IgG; 20 mg/kg) intraperitoneally every second day.

Statistical analysis

Data in figures are presented as mean \pm SEM, with *n* representing the number of experiments. One-way ANOVA with Dunnett multiple comparison, Wilcoxon, and unpaired Student *t* test were used for data analysis. Statistical significance was set at *P* value < 0.05.

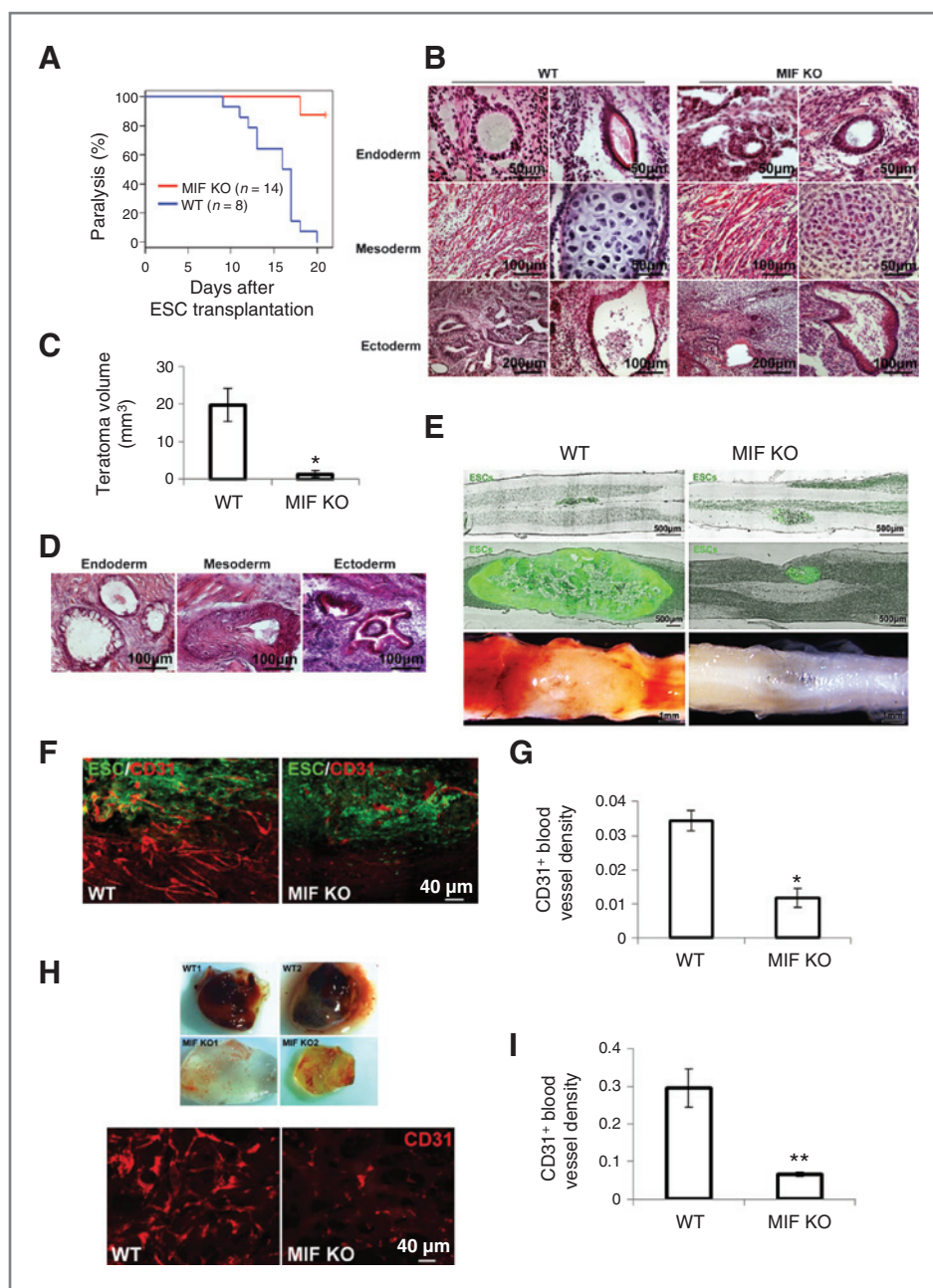
Additional methods are described in Supplementary Materials and Methods.

Results

Deletion of MIF from the host but not from ESCs inhibits teratoma growth

Undifferentiated EGFP-ESCs were stereotaxically injected into the spinal cord of mice exposed by a T9–T10 laminectomy. During the first week after ESCs injection, hind limb function as reflected by the BMS score was normal in both WT and MIF KO mice. The BMS score in WT mice decreased rapidly 10 days after injection and reached zero (paralysis; Supplementary Fig. S1A). By comparison, the BMS score declined slowly after ESC injection in MIF KO mice (Supplementary Fig. S1A). All WT mice were paralyzed at day 19 after cell transplantation (Fig. 1A). In contrast, only one out of 14 MIF KO mice was paralyzed at day 17 (Fig. 1A). We computed the rate of decay of BMS score from days 8 to 17 with the least squares method for each mouse in both WT

Figure 1. Deletion of MIF from the host inhibits teratoma development. A, ESCs were stereotactically injected into the spinal cord in WT and MIF KO mice and hind limb paralysis was analyzed by Kaplan–Meier analysis ($P < 0.05$). B, HE staining of spinal cord at 2 weeks after ESC injection showing structures derived from 3 embryonic germ lineages in both WT and MIF KO mice. C, teratoma growth in the spinal cord from MIF KO and WT mice at 2 weeks after ESC injection ($n = 10$). D, HE staining of spinal cord at 2 weeks after injection of ESCs generated from MIF KO mice showing 3 embryonic structures. E, representative micrographs showing strong GFP expression in the spinal cord at 24 hours (top) and 2 weeks (middle) after ESC injection and blood vessel development at 2 weeks after ESC injection (bottom). A representative teratoma growth from a WT mouse (left) and MIF KO mouse (right) is displayed. F, immunostaining of CD31 (red) in WT (left) and MIF KO mice (right) at 2 weeks after ESC injection. G, quantification of CD31⁺ endothelial cells in teratomas from WT and MIF KO mice ($n = 5$). H, gross morphology of Matrigel plugs (top) excised 5 days postinjection in WT and MIF KO mice and CD31 staining (bottom). I, quantification of CD31⁺ endothelial cells in Matrigel plugs from WT and MIF KO mice ($n = 6$). *, $P < 0.05$; **, $P < 0.001$; 2-sided Wilcoxon test. Data are represented as mean \pm SEM.



and MIF KO groups. The 2-sided Wilcoxon test was employed to compare these rates ($P < 0.05$). Histologic examination revealed teratoma formation in the spinal cord as a cause of the hind limb paralysis. In both WT and MIF KO mice, the tumors consisted of structures derived from all 3 embryonic germ lineages (Fig. 1B); however, teratoma growth was significantly less pronounced in the spinal cord of MIF KO versus WT mice (Fig. 1C). These data suggest that lack of host MIF is associated with reduced teratoma growth without affecting the evident pluripotency of ESCs.

We next investigated whether the genetic deletion of MIF from ESCs influenced teratoma development. MIF-deficient

ESC lines were generated from the individual blastocysts of MIF KO mice. Two undifferentiated MIF-deficient ESC lines (ES4 and ES15) were injected into the spinal cords of WT mice. MIF deficiency in ESCs did not affect teratoma development as all mice injected with these cells developed paralysis at a similar rate as those injected with WT ESCs and there was no difference in tumor size between mice injected with WT ESCs and MIF-deficient ESC lines (ES4 and ES15; Supplementary Fig. S1B). Structures originating from 3 embryonic germ layers were also observed in MIF-deficient tumors, indicating that intrinsic MIF deficiency does not affect ESC pluripotency (Fig. 1D).

Angiogenesis is restricted in MIF KO mice

Because angiogenesis is essential for embryonic development, we hypothesize that the rapid teratoma formation in WT mice depends on enhanced angiogenesis. ESCs were injected into the spinal cord and images were taken at 24 hours and 2 week after cell transplantation, respectively. Figure 1E shows the ESCs grew quickly in the WT compared with those in MIF KO mice. Furthermore, newly formed blood vessels were significantly more abundant in teratomas obtained from WT mice compared with those from MIF KO mice (Fig. 1E). We stained teratomas grown either in WT or MIF KO mice, for CD31, a marker of endothelial cells. Teratomas from WT mice had more blood vessels compared with those from MIF KO mice (Fig. 1F). By contrast, injection of PBS alone in the spinal cord did not produce neovascularization in WT or MIF KO mice (data not shown). Blood vessel density was quantified by counting the area of vessels per unit area (μm^2) across entire teratoma sections. The ratio of vessel area/tumor area was significantly higher in teratomas from WT mice compared with teratomas from MIF KO mice (Fig. 1G).

To further explore the role of MIF in neovascularization *in vivo*, MIF KO and WT mice were injected subcutaneously with Matrigel mixed with VEGF or PBS and the Matrigel plugs were excised at 5 days after implantation. Plugs mixed with VEGF from MIF KO mice were transparent, while those arising from WT mice were reddish in color, indicating a more pronounced angiogenic response in WT mice (Fig. 1H). Angiogenesis was further shown by staining of the Matrigel sections with CD31 antibody. MIF KO mice exhibited a clear and significant decrease in blood vessel density when compared with WT mice (Fig. 1I). By contrast, plugs with PBS alone did not show obvious angiogenic response in both WT and MIF KO mice (Supplementary Fig. S1C and S1D).

Teratoma angiogenesis does not require BM-derived EC progenitor cells

Confocal microscopy showed that the CD31⁺ endothelial cells present in teratomas originated from the host and not from ESC differentiation, as evidenced by their negativity for GFP (Fig. 2A). To assess whether the recruitment of BM-derived endothelial cells is required for teratoma growth, we lethally irradiated WT mice and transplanted red fluorescent BM cells from C57BL/6-Tg(ACTB-mRFP1)1F1Hadj/J⁺RFP mice.²³ ESCs then were injected into the spinal cord of these RFP-BM reconstituted mice at 4 weeks after BM replacement. Teratomas developed after 2 weeks of ESC injection. The CD31⁺ endothelial cells did not colocalize with RFP⁺ cells in the teratoma (Fig. 2B), indicating that the endothelial cells present in newly formed blood vessels were neither differentiated from ESCs nor from BM-derived cells. They were from preexisting endothelial cell proliferation.

ESCs differentiate into pericytes and pericyte coverage is restricted in MIF KO mice

Angiogenesis not only requires endothelial cell proliferation but also depends on pericytes that support vessel stabilization and maturation (22). The origin of pericytes and the molecular mechanisms that regulate their differentiation are not well

understood, however. We therefore assessed whether the pericytes present in the teratoma vasculature came from host tissue or from the differentiation of ESCs themselves. This was determined by expression of the pericyte marker NG2 and its localization to capillary vessels. Blood vessels in teratomas from WT mice had abundant NG2⁺ pericytes that appeared closely apposed to the capillaries (Fig. 2C). In contrast, the blood vessels in teratomas from MIF KO mice were covered only sparsely by pericytes (Fig. 2C), suggesting that pericyte association with endothelium is regulated by MIF. Quantitative analysis showed a significant decrease in NG2⁺ pericyte counts in MIF KO teratomas compared with WT (Fig. 2D). The pericyte density of vessels, as determined by the total number of pericytes divided by the density of CD31⁺ vessels, was significantly higher in teratomas from WT mice than from MIF KO mice (Fig. 2D). Moreover, NG2⁺ pericytes in WT and MIF KO mice were derived in part from both host and the transplanted ESCs because a portion of these cells were GFP positive (Fig. 2E). These results suggest that MIF plays a role in teratoma angiogenesis by regulating the recruitment/differentiation of pericytes from ESCs and host cells.

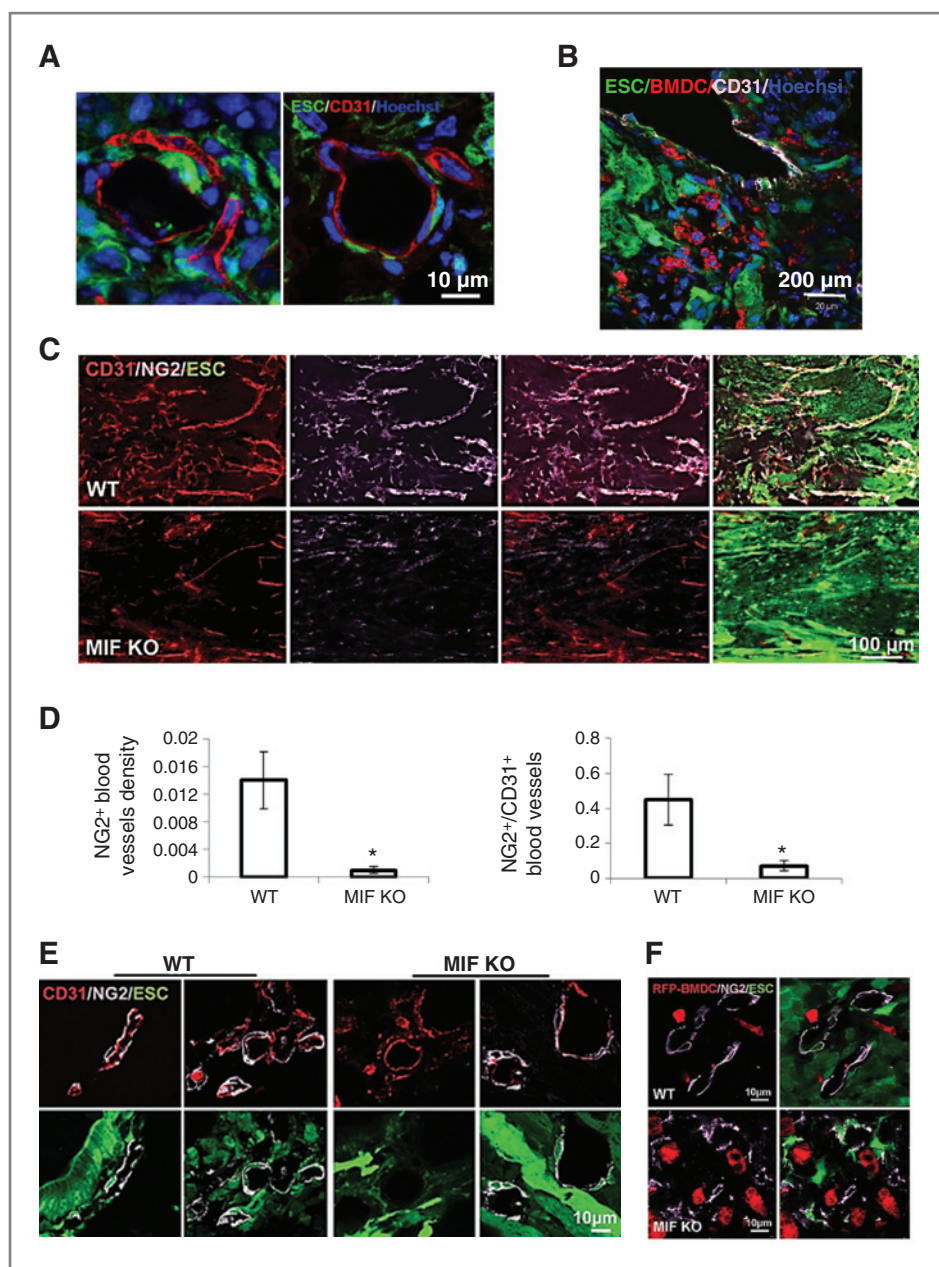
We also explored whether BM is the source of the pericyte progenitors in newly formed teratoma vessels as it is accepted that BM cells give rise to pericyte precursor cells (23). ESCs were injected into the spinal cord of RFP-BM reconstituted mice at 4 weeks after BM replacement. We observed that RFP⁺ BM cells were not positive for NG2 staining in teratomas from either WT or MIF KO mice (Fig. 2F). Taken together, our results suggest that teratoma angiogenesis does not require BM-derived endothelial cells or pericytes and that non-BM-derived progenitors contribute to teratoma vascularization.

ESCs recruit BMDMs

We next examined the cellular microenvironment that develops immediately after ESC implantation into spinal cord. By the macrophage specific-markers IBA-1 and F4/80, we found macrophages in the WT spinal cord as early as the first day after ESC injection with peak macrophage infiltration occurring after 1 to 2 weeks (Fig. 3A). Notably, there was a significant reduction in macrophage infiltration when MIF-KO mice were compared with WT mice. The mean density of macrophages (IBA-1⁺) recruited to the ESC injection site at 1 day in MIF KO mice was 0.18 ± 0.09 versus 2.55 ± 1.24 in WT mice ($n = 10$, $P < 0.05$). A similar pattern was observed at 2 weeks after ESC injection (Fig. 3A and B). Both percentages of IBA-1⁺ and F4/80⁺ macrophages were significantly higher in WT mice compared with MIF KO mice. By contrast, surgery alone (injection of PBS) did not cause evident macrophage infiltration in both WT and MIF KO mice (data not shown). It has been shown that MIF receptor CD74 (24) contributes to MIF mediated macrophage recruitment (25) and MIF may also act as a noncanonical ligand for CXCR2 and CXCR4 (26) and further attract CXCR2⁺ and CXCR4⁺ macrophages. We showed that majority of infiltrated macrophages were CD74 (Fig. 3C) and CCR2 positive (Fig. 3D). Only a small portion of macrophages were CXCR4 and CXCR2 positive during teratoma development (Supplementary Fig. S2). Furthermore, teratomas from WT mice had more CD74⁺ and CCR2⁺

Figure 2. The origin of endothelial cells and pericytes during teratoma development in WT mice at 2 weeks after ESC injection.

A, immunofluorescence staining for CD31 (red) with confocal microscope. B, representative photographs of immunostaining for CD31 (purple) in teratoma sections from WT mice after RFP⁺ BM cell transplantation. C, immunostaining of sections from WT (top) and MIF KO mice (bottom) at 2 weeks after ESC injection showing double staining for NG2 (purple) and CD31 (red). D, quantification of NG2⁺ pericyte density (left), and normalized pericyte density of vessels (right), density of pericytes divided by the density of CD31⁺ vessels ($n = 10$; *, $P < 0.05$, 2-sided Wilcoxon test). Data are represented as mean \pm SEM. E, representative confocal microscopic images of CD31/NG2 double-stained vessels within teratomas of WT (left) and MIF KO mice (right) at 2 weeks after ESC injection. F, representative confocal microscopic images of NG2⁺ pericytes (purple) and RFP⁺ BM-derived cells (red) within teratomas of WT (top) and MIF KO mice (bottom) that received RFP⁺ BM transplantation.



macrophages than those from MIF KO mice. Therefore, ESC-induced macrophage infiltration seems to be CD74/CCR2 dependent but CXCR4/2 independent.

To determine whether the macrophages within these sites represented locally activated microglia or BM-derived cell infiltration, the ESCs were injected into the spinal cord of RFP-BM reconstituted mice at 4 weeks after BM replacement and the spinal cords were examined at 2 weeks after ESC injection. Most RFP⁺ cells were IBA-1 or F4/80 positive within the teratoma tissue, suggesting that these BM-derived cells were macrophages (Fig. 3E). In other words, most IBA-1- or F4/80-positive cells colocalized with RFP⁺ cells, and we did not observe many F4/80⁺/IBA-1⁺ but RFP⁻ cells in the teratomas,

indicating that most macrophages in the teratomas are derived from BM-derived cells rather than locally activated microglia cells.

ESCs induce alternative activation of macrophages (M2 activation)

We next investigated the potential mechanisms of macrophage-ESC interaction affecting teratoma development. The M2 macrophage phenotype ("alternatively-activated" macrophages) is proangiogenic and tumor promoting (27, 28). To assess whether ESCs are able to activate infiltrated macrophages and skew them toward an M2 phenotype, we exposed mature BMDMs to conditioned medium obtained from ESC

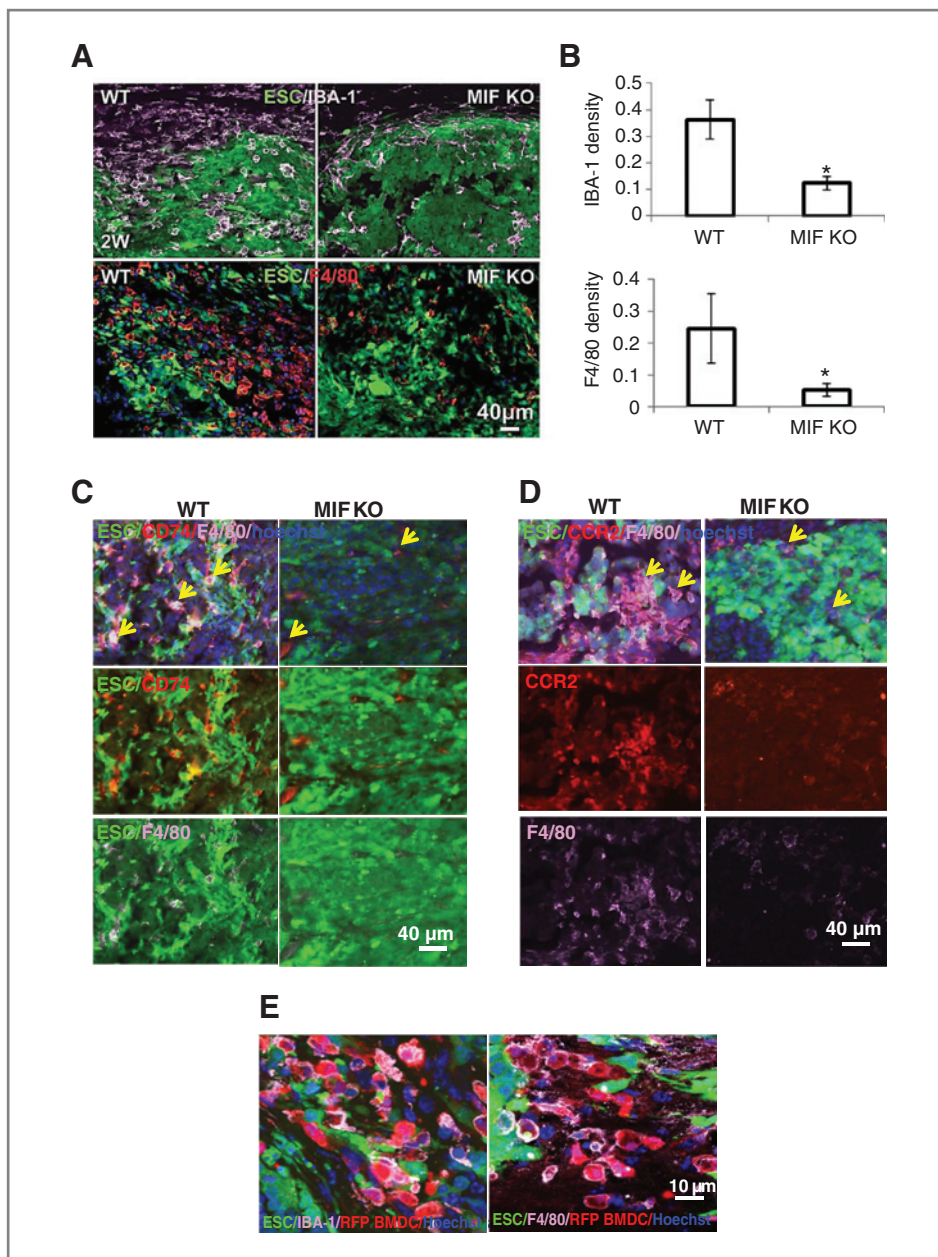
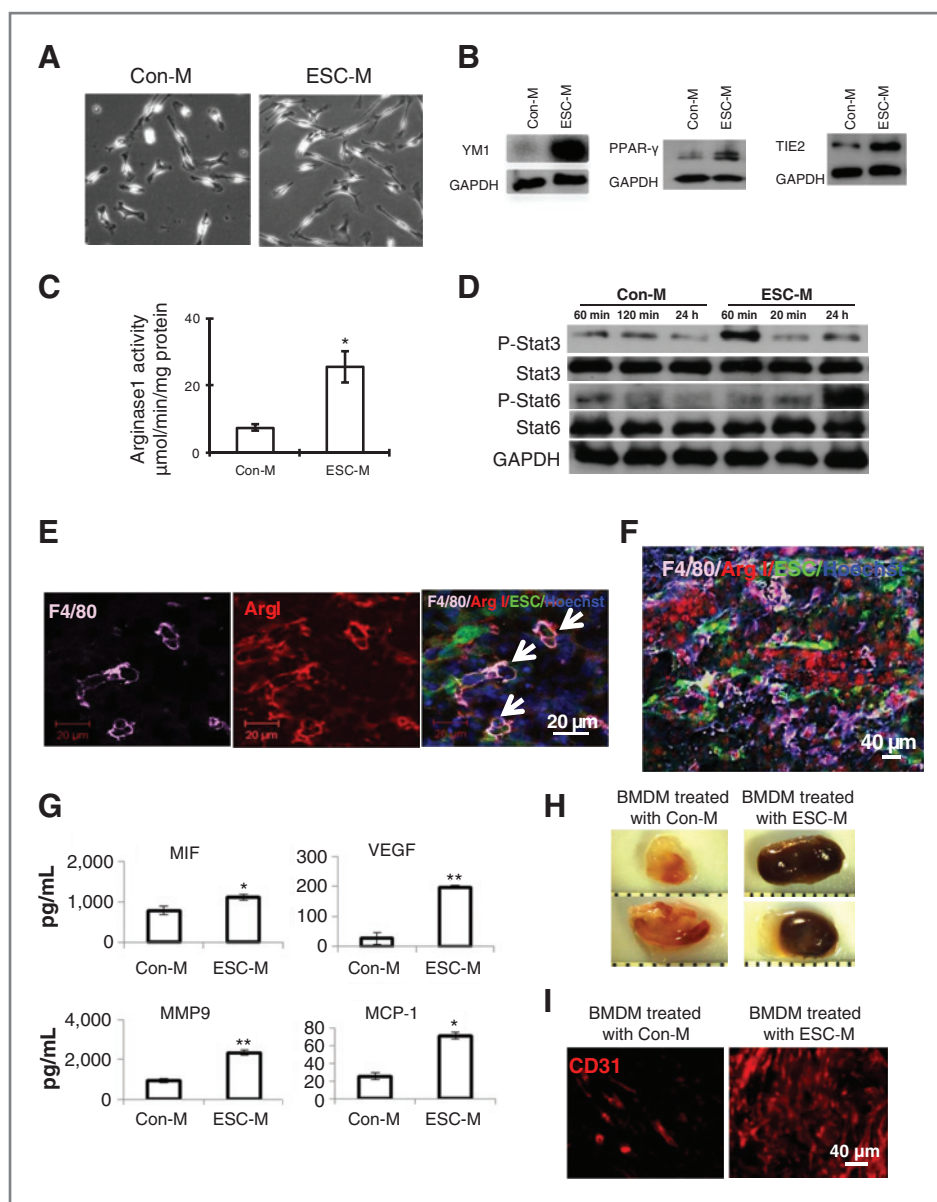


Figure 3. ESCs recruit BMDMs. A, macrophage recruitment during teratoma progression. Macrophages in the sections of spinal cord at 2 weeks after ESC transplantation in WT (left) and MIF KO mice (right) were detected by antibodies to IBA-1 (top) and F4/80 (bottom) at 2 weeks after ESC transplantation ($n = 10$; *, $P < 0.05$, 2-sided Wilcoxon test). Data are represented as mean \pm SEM. B, quantification of IBA-1⁺ macrophages (top) and F4/80⁺ (bottom) at 2 weeks after ESC transplantation. C, representative images of immunostaining of sections at 2 weeks after ESC injection showing double staining (arrows) for CD74 (red) and F4/80 (purple) in WT (left) and MIF KO mice (right). D, representative images of immunostaining of sections at 2 weeks after ESC injection showing double staining (arrows) for CCR2 (red) and F4/80 (purple) in WT (left) and MIF KO mice (right). E, BMDM recruitment during teratoma progression. Representative confocal microscopic images of sections of spinal cord from RFP-BM reconstituted mice at 2 weeks after injection were stained with IBA-1 (purple, left) and F4/80 (purple, right), respectively.

culture (ESC-M; without direct cell-cell contact) for 48 hours in the absence of macrophage colony-stimulating factor (M-CSF) and other exogenous stimuli. Cells treated with control medium (Con-M) exhibited the typical bipolar, spindle-shaped morphology of BMDM. In contrast, in the presence of ESC-M, some of macrophages showed a long, single process or bipolar processes (Fig. 4A). In addition, well-characterized markers for M2 macrophages such as Ym1, PPAR- γ , tyrosine kinase with Ig and epidermal growth factor homology domains-2 (Tie-2), and arginase 1 (28–30) were analyzed. Treatment of BMDM with ESC-M led to a significant increase in the expression of Ym1, PPAR- γ , and Tie-2 compared with BMDM cultured with Con-M alone

(Fig. 4B). To confirm that an M2 macrophage population is induced by ESCs, we measured arginase 1 activity using a colorimetric assay that detects production of urea. Treatment with ESC-M for 2 days significantly upregulated (5.4-fold increase) arginase 1 activity in BMDM, compared with treatment with Con-M (Fig. 4C). This suggests that soluble factors produced by ESCs shift macrophages toward an M2 phenotype. Because M-CSF, interleukin (IL)-13, and IL-4 drive M2 macrophage phenotype (31), we determined whether these cytokines were expressed by ESCs and thereby elicit M2 polarization. M-CSF, IL-13, and IL-4 in ESC-M were not detectable (Table 1) and ESC-M did not stimulate macrophages to produce M-CSF, IL-13, and IL-4 (data not

Figure 4. ESC-induced macrophage activation. **A**, phase-contrast photomicrographs of BMDM (original magnification, $\times 200$). BMDMs were cultured with Con-M and conditioned medium of ESCs (ESC-M) for 2 days. **B** and **C**, BMDMs from WT mice were incubated with Con-M or ESC-M for 48 hours and M2 markers were assessed by Western blot (**B**) or colorimetric assay to test arginase 1 activity ($n = 3$; **C**). **D**, phosphorylation of Stat3 (p-Stat3) and p-Stat6 in BMDM treated with Con-M and ESC-M. **E** and **F**, representative confocal images of immunostaining of sections from WT mice at 2 weeks after ESC injection showing double staining for Arginase 1 (red) and F4/80 (purple, arrows). **G**, MIF, VEGF, MMP-9, and MCP-1 in the supernatants of BMDM treated with Con-M and ESC-M for 24 hours detected by ELISA. The presented concentrations were equal to the original concentrations minus the amount in ESC-M. Data were expressed as mean \pm SEM and similar results were obtained from 3 independent experiments ($n = 3$). **H**, representative gross morphology of Matrigel plugs containing BMDM treated Con-M (left) or ESC-M (right) excised 5 days postinjection in WT mice. **I**, CD31 staining for endothelial cells in Matrigel plugs. *, $P < 0.05$; **, $P < 0.001$, 2-sided Wilcoxon test.



shown), suggesting that ESC-elicited M2 polarization of macrophages was M-CSF/IL-4/IL-13 independent.

M2 stimuli activate Stat3 or Stat6 which upregulates M2 gene expression and skew M2 polarization (32). We therefore examined whether Stat3/6 participated in ESC-induced M2 activation. Treatment of BMDM with ESC-M enhanced the activity of Stat3 within 60 minutes and also activated Stat6 at 24 hours after treatment (Fig. 4D). These data supported the conclusion that ESCs induced macrophage M2 activation is associated with activation of Stat3 and Stat6.

We further detected M2 macrophages *in vivo* with immunofluorescent double-labeling and confocal microscopy. Specifically, we stained teratoma sections for arginase 1 and F4/80. Some cells coexpressed F4/80 and arginase 1, suggesting these macrophages were M2 phenotype (Fig. 4E). We observed

enormous F4/80⁺/arginase 1⁺ macrophages in mice injected with ESCs (Fig. 4F), while M2 macrophages were not detected in normal spinal cord (data not shown). However, ESCs also express arginase 1, consistent with the report from Yachimovich-Cohen and colleagues (33).

ESCs induced an angiogenic switch in macrophages *in vitro* and *in vivo*

We determined the profile of angiogenic factors secreted by BMDM cocultured with ESC-M. WT BMDMs were incubated with ESC-M and expression of angiogenic factors were quantified by ELISA. In comparison with Con-M alone, exposure to ESC-M significantly induced MIF, VEGF, MMP-9, and monocyte chemoattractant protein-1 (MCP-1; Fig. 4G). MCP-1 is potent chemotactic factor and

Table 1. Molecules secreted by ESCs

Molecule	pg/mL/ 1×10^6 cells
VEGF	183.40 \pm 11.29
MMP-9	304.19 \pm 18.41
MCP-1	11.10 \pm 1.82
IL-1 β	Not detected
IL-4	Not detected
IL-10	Not detected
IL-12	Not detected
IL-13	Not detected
TNF- α	Not detected
M-CSF	Not detected
GM-CSF	Not detected

NOTE: ESCs were cultured for 48 hours and the molecules in the supernatants were detected by ELISA. Data were expressed as mean \pm SEM, and similar results were obtained from 3 independent experiments.

Abbreviation: GM-CSF, granulocyte-macrophage colony-stimulating factor.

contributes directly to tumor angiogenesis by a mechanism independent of monocyte recruitment (34). ESC-M also markedly increased Tie-2 (Fig. 4B). Although recruited to tumors in lower numbers than tumor-associated macrophages, Tie-2-expressing monocytes share several characteristics with M2 macrophages (35) and are a more potent source of proangiogenic signals (36). As VEGF, MIF, MMP-9, MCP-1, and Tie-2 are well-known angiogenic factors (37, 38) and ESC-M significantly increased the expression of these factors, we further evaluated the role of ESC-macrophage interaction *in vivo* by Matrigel plug assay. BMDMs containing plugs with ESC-M or Con-M were implanted subcutaneously in WT mice. As shown in Fig. 4H, 5 days after injection into mice, Matrigel plugs containing BMDM treated with ESC-M appeared much darker and were filled with blood, indicating that functional vasculature had formed via angiogenesis triggered by ESCs. In contrast, BMDMs in Con-M did not induce obvious angiogenesis (Fig. 4H). Examination of CD31 in excised Matrigel plugs revealed dramatically more extensive vessel networks in plugs containing ESC-M than in plugs without ESC-M (Fig. 4I). Our data clearly indicated that ESCs govern an angiogenic switch in macrophages *in vitro* and *in vivo*.

Macrophages enhance proliferation of endothelial cells and ESCs via production of MIF

Macrophages are an important source of MIF (39), and we showed that significant macrophages infiltrated into the sites of ESC injection (Fig. 3A). We also showed that deletion of MIF from ESCs did not block teratoma development (Supplementary Fig. S1B). We therefore hypothesized that infiltrating macrophages deliver substantial amounts of MIF into ESC niches that then supports teratoma growth. We compared MIF production from BMDMs and ESCs *in vitro* and observed that over a period of 48 hours, macrophages secreted 34.63 ± 2.50

ng/mL MIF per million cells (Fig. 5A), while 1.23 ± 0.06 ng/mL MIF was produced by same number ESCs. These data indicate that macrophages are a major source of MIF; accordingly, we reasoned that infiltrating macrophages may deliver MIF into ESC niches to impart a direct effect on endothelial cells or ESCs. To address this point, endothelial cells were incubated with recombinant mouse MIF (rMIF) and their proliferation was assessed. We ran the least squares regression to see whether there is a linear trend on the dose effect. The *P* value was 0 with degree of freedom 47 and the multiple R^2 was 0.3484, revealing that MIF stimulates endothelial cell proliferation in a dose-dependent manner (Fig. 5B). Moreover, when endothelial cells were cultured with the macrophage conditioned medium from WT or MIF KO mice, the medium from the WT macrophages caused a $90.10\% \pm 10.60\%$ increase above control in endothelial cell proliferation, while medium from MIF KO macrophages did not significantly stimulate proliferation. In addition, inhibition of MIF activity by ISO-1, a small-molecule inhibitor of MIF (40), by pretreatment of medium from WT macrophages significantly suppressed macrophage-induced endothelial cell proliferation (Fig. 5C). We also showed that rMIF and WT macrophage conditioned medium significantly enhanced proliferation of primary endothelial cells from MIF KO mice, whereas ISO-1 decreased MIF activity (Fig. 5D), suggesting that cell proliferation could be rescued in the MIF KO group by the addition of rMIF. These data suggest that macrophages are a major source of the MIF that supports angiogenesis. In addition to stimulated endothelial cell proliferation, rMIF or medium from WT macrophages also enhanced ESC proliferation (Fig. 5E and F), and inhibition of MIF by ISO-1 reduced macrophage-induced ESC proliferation (Fig. 5F).

BM-derived cells produce MIF that contributes to teratoma angiogenesis and growth

We showed that macrophages infiltrating into teratomas are derived from the BM and produce significant amounts of MIF that directly stimulate endothelial cell and ESC proliferation. To better substantiate that BM-derived cells are indeed the major producer of MIF within ESC niches *in vivo*, ESCs were injected into the lethally irradiated MIF KO mice that had been previously reconstituted with WT BM (WT \rightarrow KO mice; Fig. 6A). The appearance and timing of teratoma formation in these mice were similar to that observed in fully WT host mice. Furthermore, the teratomas appeared hemorrhagic in WT \rightarrow KO mice (Fig. 6B) and grew significantly faster than those in the MIF KO mice that had not undergone BM transplantation (Fig. 6C), suggesting that transplantation of WT BM-derived cells in MIF KO mice restored teratoma development.

We also investigated whether BM-derived cells from MIF KO mice are sufficient to suppress teratoma development by ESCs implanted into WT mice. We lethally irradiated WT mice and reconstituted their BM with either BM cells from WT (WT \rightarrow WT) or MIF KO (KO \rightarrow WT) mice (Fig. 6A). The chimeric KO \rightarrow WT mice showed decreased angiogenesis and reduced teratoma growth when compared with chimeric WT \rightarrow WT mice (Fig. 6B and C). Furthermore, rMIF administration (20

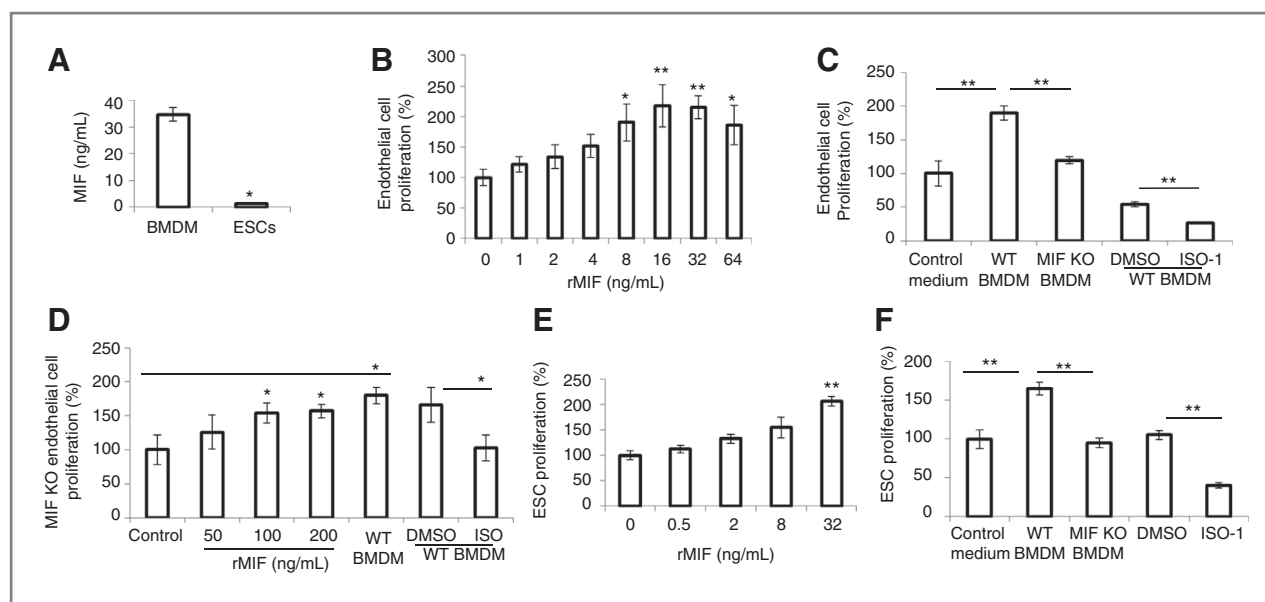


Figure 5. Macrophages enhance proliferation of endothelial cells and ESCs via production of MIF. A, secretion of MIF into culture supernatants of BMDM or ESCs as measured by ELISA. Supernatants were collected after 48 hours, and the values expressed as ng/mL per million cells ($n = 3$; $P < 0.05$, Student *t* test). B, effect of MIF on endothelial cell proliferation. Endothelial cells were incubated with rMIF at the indicated concentration for 3 days and cell proliferation was assessed by SRB assay ($n = 3$; $P < 0.05$; $**$, $P < 0.001$, ANOVA). C, effect of conditioned macrophage medium on endothelial cell proliferation. Endothelial cells were incubated with control medium, conditioned WT macrophage medium (WT BMDM), conditioned MIF KO macrophage medium (MIF KO BMDM), WT BMDM pretreated with DMSO or ISO-1 (500 nmol/L), respectively ($n = 3$; $**$, $P < 0.001$, ANOVA). D, effect of rMIF on proliferation of endothelial cell from MIF KO mice. Primary endothelial cells from MIF KO mice were incubated with rMIF, WT BMDM, WT BMDM pretreated with DMSO or ISO-1 (250 nmol/L), respectively for 3 days ($n = 3$; $*$, $P < 0.05$, ANOVA). E, effect of MIF on ESC proliferation. ESCs were incubated with rMIF at the indicated concentration for 3 days ($n = 3$; $**$, $P < 0.001$, ANOVA). F, effect of conditioned macrophage medium on ESC proliferation. ESCs were incubated with control medium, WT BMDM, MIF KO BMDM, WT BMDM pretreated with DMSO and or ISO-1 (500 nmol/L), respectively ($n = 3$; $**$, $P < 0.001$, ANOVA). All data are represented as means \pm SEM of 3 independent experiments done in duplicate.

$\mu\text{g}/\text{mice}/\text{wk}$, i.p. restored teratoma development in KO \rightarrow WT mice (Supplementary Fig. S3A). This result indicates that deletion of MIF expression in hematopoietic cells is sufficient to inhibit teratoma development.

Teratoma development outside of spinal cord

To better exclude the effect of neighboring neural and glial cells on teratoma growth and differentiation, an examination of teratomas induced by ESC transplantation in nonneural sites could support the role of signals produced by macrophages versus other tissue types. ESCs were injected into liver and leg muscle of WT and MIF KO mice, respectively, and representative sets of teratoma that developed in each group at week 3 are shown in Supplementary Fig. S3B and S3C. Teratomas that developed after ESC injection were significantly smaller in the MIF KO mice compared with those in WT mice. By 3 weeks after injection, the mean teratoma size in the liver and muscle was 5.5% and 36.6% smaller in MIF KO mice than WT mice ($n = 8$, $P < 0.05$). These results not only confirmed that MIF is crucial for teratoma development but also excluded the role of resident cells in the spinal cord in teratoma development.

Targeting MIF pharmacologically inhibits teratoma growth

On the basis of the above observations, we reasoned that selective inhibition of MIF activity would inhibit angiogenesis

and teratoma growth. Mice that received an injection of ESCs were randomized into 3 groups. A sham group only received ESC injection without further treatment. Mice in the treatment groups were administered a neutralizing anti-MIF mAb or an isotype control antibody only by injection i.p. at a dose of 20 mg/kg q.o.d. (every other day). As shown in Fig. 6D–G, mice that received anti-MIF showed a significant inhibition of blood vessel formation and teratoma progression, with a mean teratoma size of $6.88 \pm 1.84 \text{ mm}^3$ in the anti-MIF group versus $23.01 \pm 5.40 \text{ mm}^3$ in the control IgG₁ group ($n = 8$, $P < 0.05$). Moreover, the anti-MIF-treated mice teratomas had fewer numbers of CD31-positive vessels than those from the control IgG₁-treated mice and sham group (Fig. 6G).

Discussion

Inflammatory cells play an important role in tumor progression (41). However, it is not clear whether ESCs have the potential to generate the inflammatory environment necessary for supporting their growth. This is the first study to show that syngeneic ESC transplantation provokes an inflammatory response that involves the rapid recruitment of BMDMs and alternative macrophage activation. The BMDMs create a microenvironment that facilitates the initiation and progression of teratomas. This involves the release of MIF and other angiogenic factors to promote the formation of new capillaries from preexisting vessels. Our data indicate that MIF released

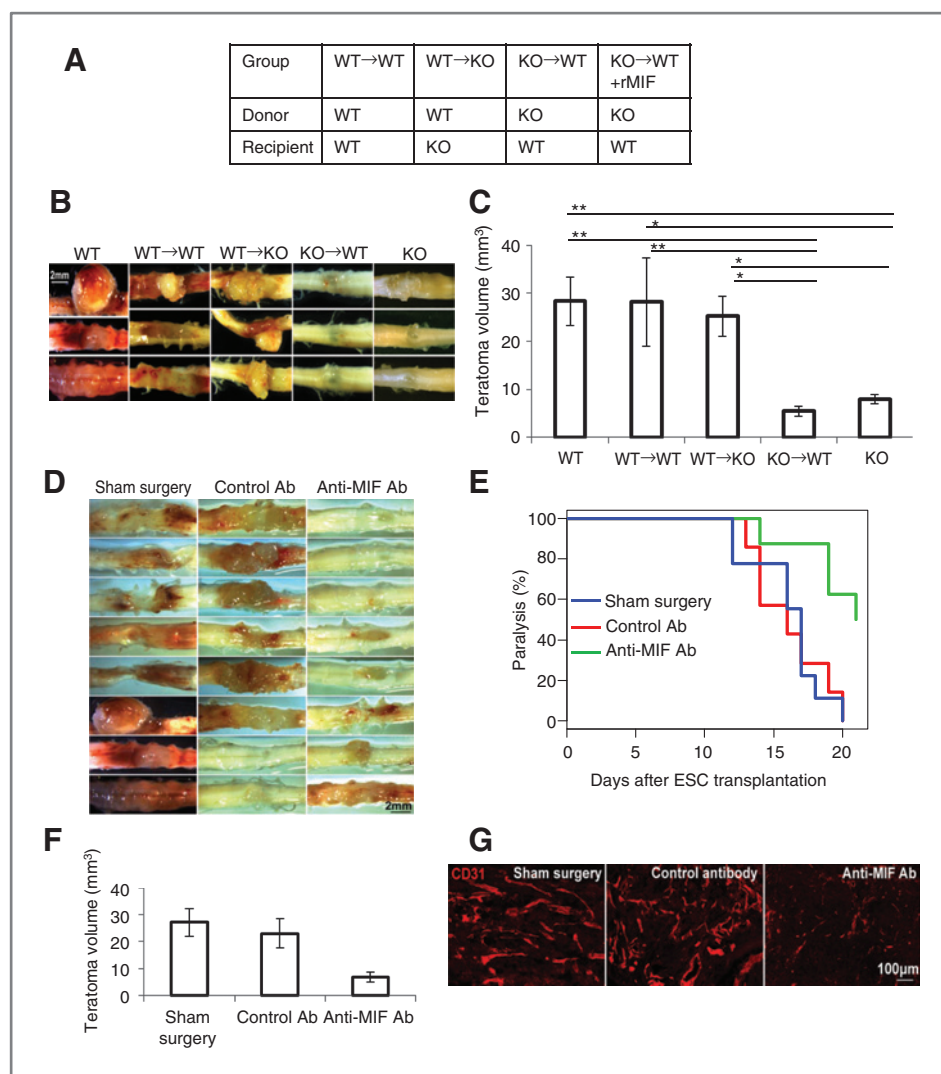


Figure 6. BM-derived cells produce MIF that contributes to teratoma growth and targeting MIF suppresses teratoma growth. A, groups of mice used for BM reconstitution. ESCs were injected into the spinal cord in 5 groups of mice (WT, MIF KO, WT→WT, WT→KO, KO→WT). B, representative images of teratomas in the spinal cord harvested from the indicated groups at 3 weeks after ESC transplantation. C, average teratoma size at 3 weeks after ESC transplantation from the indicated groups ($n = 4$; *, $P < 0.05$; **, $P < 0.001$, ANOVA). D, representative images of teratomas harvested from control groups (sham surgery and control antibody) and treated group (anti-MIF mAb) at 3 weeks after ESC transplantation. E, Kaplan-Meier analysis was used to indicate limb paralysis in control and treated groups ($n = 8$). F, average teratoma size at 3 weeks after ESC transplantation in the indicated groups ($n = 8$; *, $P < 0.05$, ANOVA). Data are represented as mean \pm SEM. G, representative photographs of teratoma sections at 3 weeks postinjection revealing CD31 staining in sham surgery group, control antibody-treated group, and anti-MIF mAb-treated group.

by BMDMs is both necessary and sufficient to drive angiogenesis and support teratoma progression and lead to the conclusion that MIF is a key regulator in the link between inflammation and teratoma development. Although ESCs are not oncogenically transformed, they still have the ability to recruit BM-derived cells. How are these BMDMs recruited by ESCs? It was reported that MIF receptor CD74 (24) contributes to MIF-mediated macrophage recruitment (25) and MIF also acts as a noncanonical ligand for CXCR2 and CXCR4 (26) and further attract CXCR2⁺ and CXCR4⁺ macrophages. We showed that majority of infiltrated macrophages were CD74 positive and only a small portion of macrophages were CXCR4 and CXCR2 positive during teratoma development, suggesting that ESC-induced macrophage infiltration may be CD74 dependent but CXCR4/2 independent. MCP-1 or CCL2 is an essential chemokine, which acts through its receptor CCR2 to induce the migration and activation of macrophages and thus tumor progression (42). We showed that ESCs express MCP-1 (Table 1) and infiltrated macrophages express CCR2 (Fig. 3D), suggesting that ESC-produced MCP-1 is involved in macro-

phage accumulation via CCR2. It has been reported that MIF-deficient macrophages and endothelial cells (host MIF deficiency) showed reduced leukocyte-endothelial interaction. Absence of local MIF markedly reduces macrophage chemotactic response to MCP-1 both *in vitro* and *in vivo* (25, 43). MIF deficiency also reduced basal expression of E-selectin, VCAM-1, and ICAM-1 (44). These data suggest that in the presence of MCP-1 (expressed by ESCs), WT macrophages are able to interact with endothelial cells and infiltrate in response to MCP-1. However, macrophage-endothelial interaction is impaired in MIF KO mice and the chemotactic response to MCP-1 was diminished. This may explain why MIF expression from host but not from ESCs is responsible for ESC-induced macrophage recruitment. Once present in the ESC injection site, ESCs induce these cells to express more MCP-1, VEGF, and MMP-9 and to attract more macrophages. However, more detailed studies will be necessary to determine whether additional molecules either alone or in combination contribute to macrophage recruitment to the site of ESC implantation.

Macrophages are a heterogeneous population of myeloid-derived cells and are categorized as classically activated (M1) or alternatively activated (M2; ref. 31). M2 type macrophages support tumor survival, growth, and metastasis and seem to play a role in tumor angiogenesis and immune evasion (27). Many questions, however, still await answers. It would be interesting to know whether and how stem cells induce a phenotype switch in infiltrated macrophages. Our results showed for the first time that ESCs produced soluble factors that not only induced the macrophage accumulation but also play an essential role in macrophage M2 activation. However, we found that M-CSF, IL-4, and IL-13, 3 well-documented cytokines that drive M2 macrophage differentiation (31), were not involved in ESC-induced macrophage M2 polarization. Further studies are needed to determine the molecular mechanisms of ESC regulating macrophage polarization.

BM-derived cells have been shown to play an important role in tumor neovascularization and the recruitment of BM-derived endothelial and pericyte progenitors participates in tumor vascular development (45). This study shows that angiogenesis during ESC proliferation and teratoma progression does not require the contribution of BM-derived endothelial, ESC-differentiated endothelial cells, or BM-derived pericyte progenitors. These results are consistent with Purhonen and colleagues who observed that BM-derived cells do not contribute to vascular endothelium and are not needed for tumor growth (46). We showed that BM-derived cells directly contribute to teratoma vascular development through one major mechanism, that is, the delivery of MIF and other factors. Infiltrated macrophages produce appreciable amounts of MIF that not only regulate angiogenesis by directly interacting with endothelial cells but also enhance ESC proliferation. In addition to producing MIF, macrophages promote angiogenesis and tissue remodeling by the secretion of VEGF and MMP-9 (37, 47, 48). MMP-9 produced by BM-derived cells initiates the angiogenic switch leading to tumor growth and progression (37, 49). It has been shown that MIF directly induces expression of MCP-1, MMP-9, and VEGF in different types of cells (16, 50).

Targeting MIF may also suppress release of MCP-1, VEGF, and MMP-9, thereby inhibiting angiogenesis and impairing teratoma growth.

In conclusion, the microenvironment niches of ESCs are crucial for teratoma initiation and progression. ESCs produce chemokines such as MCP-1 induce the infiltration of macrophages and then induce M2 activation. These activated macrophages express multiple angiogenic growth factors and proteinases that promote angiogenesis. A better understanding of the regulation and function of different types of cells in the tumorigenicity of ESCs may yield useful therapies for the safe transplantation of ESCs. In addition to inhibiting MIF expression, the targeting of the host microenvironment of the transplantation site rather than ESCs directly could be a more efficient approach for suppressing angiogenesis and teratoma progression without affecting the pluripotency of ESCs. It is of further interest that human *mif* is encoded by a functionally polymorphic locus (51, 52) and that *mif* promoter polymorphisms that are associated with increased systemic MIF expression have been linked to increased clinical disease severity (52, 53). Thus, teratoma development also may have an important genetic basis that could affect the clinical selection of patients for therapy.

Disclosure of Potential Conflicts of Interest

R. Bucala is a coinventor on patents describing MIF inhibitors. No potential conflicts of interest were disclosed by the other authors.

Acknowledgments

The authors thank Dr. M. Schachner for providing mouse EGFP-ESCs and help from Dr. N. Goldsmith, Dr. X. Sun, and Dr. YX. Chen from the W.M. Keck Center for Collaborative Neuroscience.

Grant Support

This work was supported by the National Science Foundation (DMS-0714589), NIH (R01 GM100474-01), a Joyce and Les Goodman scholarship, and the New Jersey Commission on Spinal Cord Research (07-3068-SCR-E-0).

The costs of publication of this article were defrayed in part by the payment of page charges. This article must therefore be hereby marked *advertisement* in accordance with 18 U.S.C. Section 1734 solely to indicate this fact.

Received September 27, 2011; revised February 17, 2012; accepted March 15, 2012; published OnlineFirst March 29, 2012.

References

- Roy NS, Cleren C, Singh SK, Yang L, Beal MF, Goldman SA. Functional engraftment of human ES cell-derived dopaminergic neurons enriched by coculture with telomerase-immortalized midbrain astrocytes. *Nat Med* 2006;12:1259-68.
- Yang D, Zhang ZJ, Oldenburg M, Ayala M, Zhang SC. Human embryonic stem cell-derived dopaminergic neurons reverse functional deficit in parkinsonian rats. *Stem Cells* 2008;26:55-63.
- Dressel R, Schindehutte J, Kuhlmann T, Elsner L, Novota P, Baier PC, et al. The tumorigenicity of mouse embryonic stem cells and *in vitro* differentiated neuronal cells is controlled by the recipients' immune response. *PLoS One* 2008;3:e2622.
- Fair JH, Cairns BA, Lapaglia MA, Caballero M, Pleasant WA, Hatada S, et al. Correction of factor IX deficiency in mice by embryonic stem cells differentiated *in vitro*. *Proc Natl Acad Sci U S A* 2005;102:2958-63.
- Nussbaum J, Minami E, Laflamme MA, Virag JA, Ware CB, Masino A, et al. Transplantation of undifferentiated murine embryonic stem cells in the heart: teratoma formation and immune response. *FASEB J* 2007;21:1345-57.
- Okita K, Nakagawa M, Hyenjong H, Ichisaka T, Yamanaka S. Generation of mouse induced pluripotent stem cells without viral vectors. *Science* 2008;322:949-53.
- Tsuji O, Miura K, Okada Y, Fujiyoshi K, Mukaino M, Nagoshi N, et al. Therapeutic potential of appropriately evaluated safe-induced pluripotent stem cells for spinal cord injury. *Proc Natl Acad Sci U S A* 2010;107:12704-9.
- Miura K, Okada Y, Aoi T, Okada A, Takahashi K, Okita K, et al. Variation in the safety of induced pluripotent stem cell lines. *Nat Biotechnol* 2009;27:743-5.
- Goldring CE, Duffy PA, Benvenisty N, Andrews PW, Ben-David U, Eakins R, et al. Assessing the safety of stem cell therapeutics. *Cell Stem Cell* 2011;8:618-28.
- Ben-David U, Benvenisty N. The tumorigenicity of human embryonic and induced pluripotent stem cells. *Nat Rev Cancer* 2011;11:268-77.
- Blum B, Benvenisty N. The tumorigenicity of diploid and aneuploid human pluripotent stem cells. *Cell Cycle* 2009;8:3822-30.
- Blum B, Benvenisty N. The tumorigenicity of human embryonic stem cells. *Adv Cancer Res* 2008;100:133-58.

13. Blum B, Bar-Nur O, Golan-Lev T, Benvenisty N. The anti-apoptotic gene survivin contributes to teratoma formation by human embryonic stem cells. *Nat Biotechnol* 2009;27:281-7.
14. Bucala R, Donnelly SC. Macrophage migration inhibitory factor: a probable link between inflammation and cancer. *Immunity* 2007;26:281-5.
15. Ren Y, Chan HM, Fan J, Xie Y, Chen YX, Li W, et al. Inhibition of tumor growth and metastasis *in vitro* and *in vivo* by targeting macrophage migration inhibitory factor in human neuroblastoma. *Oncogene* 2006;25:3501-8.
16. Ren Y, Tsui HT, Poon RT, Ng IO, Li Z, Chen Y, et al. Macrophage migration inhibitory factor: roles in regulating tumor cell migration and expression of angiogenic factors in hepatocellular carcinoma. *Int J Cancer* 2003;107:22-9.
17. Bozza M, Satoskar AR, Lin G, Lu B, Humbles AA, Gerard C, et al. Targeted disruption of migration inhibitory factor gene reveals its critical role in sepsis. *J Exp Med* 1999;189:341-6.
18. Chen J, Bernreuther C, Dihne M, Schachner M. Cell adhesion molecule I1-transfected embryonic stem cells with enhanced survival support regrowth of corticospinal tract axons in mice after spinal cord injury. *J Neurotrauma* 2005;22:896-906.
19. Ren Y, Stuart L, Lindberg FP, Rosenkranz AR, Chen Y, Mayadas TN, et al. Nonphlogistic clearance of late apoptotic neutrophils by macrophages: efficient phagocytosis independent of beta 2 integrins. *J Immunol* 2001;166:4743-50.
20. Engesser-Cesar C, Anderson AJ, Basso DM, Edgerton VR, Cotman CW. Voluntary wheel running improves recovery from a moderate spinal cord injury. *J Neurotrauma* 2005;22:157-71.
21. Chen J, Somanath PR, Razorenova O, Chen WS, Hay N, Bornstein P, et al. Akt1 regulates pathological angiogenesis, vascular maturation and permeability *in vivo*. *Nat Med* 2005;11:1188-96.
22. Gerhardt H, Betsholtz C. Endothelial-pericyte interactions in angiogenesis. *Cell Tissue Res* 2003;314:15-23.
23. Hall AP. Review of the pericyte during angiogenesis and its role in cancer and diabetic retinopathy. *Toxicol Pathol* 2006;34:763-75.
24. Leng L, Metz CN, Fang Y, Xu J, Donnelly S, Baugh J, et al. MIF signal transduction initiated by binding to CD74. *J Exp Med* 2003;197:1467-76.
25. Fan H, Hall P, Santos LL, Gregory JL, Fingerle-Rowson G, Bucala R, et al. Macrophage migration inhibitory factor and CD74 regulate macrophage chemotactic responses via MAPK and Rho GTPase. *J Immunol* 2011;186:4915-24.
26. Bernhagen J, Krohn R, Lue H, Gregory JL, Zernecke A, Koenen RR, et al. MIF is a noncognate ligand of CXC chemokine receptors in inflammatory and atherogenic cell recruitment. *Nat Med* 2007;13:587-96.
27. Pollard JW. Tumour-educated macrophages promote tumour progression and metastasis. *Nat Rev Cancer* 2004;4:71-8.
28. Sica A, Schioppa T, Mantovani A, Allavena P. Tumour-associated macrophages are a distinct M2 polarised population promoting tumour progression: potential targets of anti-cancer therapy. *Eur J Cancer* 2006;42:717-27.
29. Bouhlel MA, Derudas B, Rigamonti E, Dievart R, Brozek J, Haulon S, et al. PPARgamma activation primes human monocytes into alternative M2 macrophages with anti-inflammatory properties. *Cell Metab* 2007;6:137-43.
30. Murdoch C, Tazzyman S, Webster S, Lewis CE. Expression of Tie-2 by human monocytes and their responses to angiopoietin-2. *J Immunol* 2007;178:7405-11.
31. Gordon S. Alternative activation of macrophages. *Nat Rev Immunol* 2003;3:23-35.
32. Sica A, Bronte V. Altered macrophage differentiation and immune dysfunction in tumor development. *J Clin Invest* 2007;117:1155-66.
33. Yachimovich-Cohen N, Even-Ram S, Shufaro Y, Rachmilewitz J, Reubinoff B. Human embryonic stem cells suppress T cell responses via arginase I-dependent mechanism. *J Immunol* 2010;184:1300-8.
34. Hong KH, Ryu J, Han KH. Monocyte chemoattractant protein-1-induced angiogenesis is mediated by vascular endothelial growth factor-A. *Blood* 2005;105:1405-7.
35. Biswas SK, Mantovani A. Macrophage plasticity and interaction with lymphocyte subsets: cancer as a paradigm. *Nat Immunol* 2010;11:889-96.
36. Lewis CE, De Palma M, Naldini L. Tie2-expressing monocytes and tumor angiogenesis: regulation by hypoxia and angiopoietin-2. *Cancer Res* 2007;67:8429-32.
37. Coussens LM, Tinkle CL, Hanahan D, Werb Z. MMP-9 supplied by bone marrow-derived cells contributes to skin carcinogenesis. *Cell* 2000;103:481-90.
38. Niu J, Azfer A, Zhelyabovska O, Fatma S, Kolattukudy PE. Monocyte chemotactic protein (MCP)-1 promotes angiogenesis via a novel transcription factor, MCP-1-induced protein (MCPIP). *J Biol Chem* 2008;283:14542-51.
39. Calandra T, Bernhagen J, Mitchell RA, Bucala R. The macrophage is an important and previously unrecognized source of macrophage migration inhibitory factor. *J Exp Med* 1994;179:1895-902.
40. Lubetsky JB, Dios A, Han J, Aljabari B, Ruzsicska B, Mitchell R, et al. The tautomerase active site of macrophage migration inhibitory factor is a potential target for discovery of novel anti-inflammatory agents. *J Biol Chem* 2002;277:24976-82.
41. Coussens LM, Werb Z. Inflammation and cancer. *Nature* 2002;420:860-7.
42. Fujimoto H, Sangai T, Ishii G, Ikehara A, Nagashima T, Miyazaki M, et al. Stromal MCP-1 in mammary tumors induces tumor-associated macrophage infiltration and contributes to tumor progression. *Int J Cancer* 2009;125:1276-84.
43. Gregory JL, Morand EF, McKeown SJ, Ralph JA, Hall P, Yang YH, et al. Macrophage migration inhibitory factor induces macrophage recruitment via CC chemokine ligand 2. *J Immunol* 2006;177:8072-9.
44. Cheng Q, McKeown SJ, Santos L, Santiago FS, Khachigian LM, Morand EF, et al. Macrophage migration inhibitory factor increases leukocyte-endothelial interactions in human endothelial cells via promotion of expression of adhesion molecules. *J Immunol* 2010;185:1238-47.
45. De Palma M, Naldini L. Role of haematopoietic cells and endothelial progenitors in tumour angiogenesis. *Biochim Biophys Acta* 2006;1766:159-66.
46. Purhonen S, Palm J, Rossi D, Kaskenpaa N, Rajantie I, Yla-Herttuala S, et al. Bone marrow-derived circulating endothelial precursors do not contribute to vascular endothelium and are not needed for tumor growth. *Proc Natl Acad Sci U S A* 2008;105:6620-5.
47. Lewis JS, Landers RJ, Underwood JC, Harris AL, Lewis CE. Expression of vascular endothelial growth factor by macrophages is up-regulated in poorly vascularized areas of breast carcinomas. *J Pathol* 2000;192:150-8.
48. Huang S, Van Arsdall M, Tedjarati S, McCarty M, Wu W, Langley R, et al. Contributions of stromal metalloproteinase-9 to angiogenesis and growth of human ovarian carcinoma in mice. *J Natl Cancer Inst* 2002;94:1134-42.
49. Giraudo E, Inoue M, Hanahan D. An amino-bisphosphonate targets MMP-9-expressing macrophages and angiogenesis to impair cervical carcinogenesis. *J Clin Invest* 2004;114:623-33.
50. Kong YZ, Yu X, Tang JJ, Ouyang X, Huang XR, Fingerle-Rowson G, et al. Macrophage migration inhibitory factor induces MMP-9 expression: implications for destabilization of human atherosclerotic plaques. *Atherosclerosis* 2005;178:207-15.
51. Donn RP, Shelley E, Ollier WE, Thomson W. A novel 5'-flanking region polymorphism of macrophage migration inhibitory factor is associated with systemic-onset juvenile idiopathic arthritis. *Arthritis Rheum* 2001;44:1782-5.
52. Baugh JA, Chitnis S, Donnelly SC, Monteiro J, Lin X, Plant BJ, et al. A functional promoter polymorphism in the macrophage migration inhibitory factor (MIF) gene associated with disease severity in rheumatoid arthritis. *Genes Immun* 2002;3:170-6.
53. Radstake TR, Sweep FC, Welsing P, Franke B, Vermeulen SH, Geurts-Moespot A, et al. Correlation of rheumatoid arthritis severity with the genetic functional variants and circulating levels of macrophage migration inhibitory factor. *Arthritis Rheum* 2005;52:3020-9.

Cancer Research

The Journal of Cancer Research (1916–1930) | The American Journal of Cancer (1931–1940)

MIF Produced by Bone Marrow–Derived Macrophages Contributes to Teratoma Progression after Embryonic Stem Cell Transplantation

Xi Wang, Tianxiang Chen, Lin Leng, et al.

Cancer Res 2012;72:2867-2878. Published OnlineFirst March 29, 2012.

Updated version Access the most recent version of this article at:
doi:[10.1158/0008-5472.CAN-11-3247](https://doi.org/10.1158/0008-5472.CAN-11-3247)

Supplementary Material Access the most recent supplemental material at:
<http://cancerres.aacrjournals.org/content/suppl/2012/03/29/0008-5472.CAN-11-3247.DC1.html>

Cited Articles This article cites by 53 articles, 20 of which you can access for free at:
<http://cancerres.aacrjournals.org/content/72/11/2867.full.html#ref-list-1>

Citing articles This article has been cited by 1 HighWire-hosted articles. Access the articles at:
<http://cancerres.aacrjournals.org/content/72/11/2867.full.html#related-urls>

E-mail alerts [Sign up to receive free email-alerts](#) related to this article or journal.

Reprints and Subscriptions To order reprints of this article or to subscribe to the journal, contact the AACR Publications Department at pubs@aacr.org.

Permissions To request permission to re-use all or part of this article, contact the AACR Publications Department at permissions@aacr.org.